TECHNISCHE MECHANIK
European Journal of Engineering Mechanics
Diamond Open Access
journal homepage: www.ovgu.de/techmech

Tech. Mech., Vol. 46, Is. 3, (2026), 1–15
Received: 06.05.2026
Accepted: 01.10.2025
Available online: 19.10.2026

Electrothermoconvection in a Dielectric Navier-Stokes-Voigt Viscoelastic Fluid in Sparsely Distributed Porous Medium: Effect of Electric Field, Rotation and Internal Heat Source

Bhanu Priya[1], Harjinder Singh[2], and Jyoti Prakash[1]*

[1] Department of Mathematics and Statistics, Himachal Pradesh University, Shimla, Himachal Pradesh, 171005, India.
[2] Department of Mathematics, Kanwar Durga Chand Govt. Degree College, Jaisinghpur, Kangra, 176095, Himachal Pradesh, India.

Abstract: In the present paper, the simultaneous effect of a vertical AC electric field, rotation and an internal heat source on a dielectric viscoelastic fluid (Navier-Stokes-Voigt model) saturating a porous medium has been investigated using the Darcy-Brinkman model when heated from below or above. While the individual effects of an AC electric field, rotation and internal heating on dielectric and viscoelastic fluids have been examined separately in earlier studies, the combined influence of all three factors on a Navier–Stokes–Voigt viscoelastic dielectric fluid layer saturating a sparsely distributed porous medium has not been addressed so far, and constitutes the central novelty of the present investigation. A linear stability analysis employing the normal mode technique is conducted and the eigenvalue problem is solved exactly for free boundaries. The impact of the electric field, rotation and internal heat source on the fluid system for both stationary convection and oscillatory convection is analysed numerically and predicted graphically. It has been shown that an increase in the ratio of viscosities, the Taylor number and inverse Darcy number, enhances the stability of the Navier-Stokes-Voigt viscoelastic rotating dielectric fluid layer. However, electrical Rayleigh number has a destabilizing effect on the onset of both stationary and oscillatory convections. Moreover, the Navier–Stokes–Voigt parameter tends to destabilize the onset of oscillatory convection, while it does not affect the onset of stationary convection. It is also predicted that the system is more stable when heated from above than heated from below. Further, the results derived herein also validate the existing results in the literature. To the best of the authors' knowledge, these findings have not been previously reported.

Keywords: Navier-Stokes-Voigt, Dielectric fluid, Heat generation, Porous medium, Stationary convection, Oscillatory convection, Rotation, Darcy-Brinkman Model.

1 Introduction

In recent years, the study of non-Newtonian fluids has gained significant attention due to their widespread applications across various fields of science, engineering, and technology. Despite their presence and significance in many practical issues, non-Newtonian fluids are the subject of comparatively little research, even though electrohydrodynamic instability has been thoroughly studied in a Newtonian dielectric fluid layer. Non-Newtonian fluids, in contrast to Newtonian fluids, come in a variety of forms and are not amenable to a single approach. Foundational frameworks for viscoelastic fluids include the Oldroyd, Maxwell and Kelvin-Voigt models. However, studies on the impact of a vertical AC electric field on the beginning of convection in a viscoelastic dielectric fluid are quite limited. Othman (2001) studied the onset of convection occurring in a viscoelastic dielectric fluid layer heated from below. Othman and Sweilam (2002) examined the effect of a vertical AC electric field on the stability of natural convection, which occurs in a dielectric viscoelastic fluid between two parallel horizontal plates with internal heat generation. The effect of rotation on electrohydrodynamic instability in a layer of viscoelastic dielectric fluid heated from below has been considered by Othman and Zaki (2003). El-Sayed (2008) has analysed the onset of electrohydrodynamic instability in a horizontal layer of Oldroydian viscoelastic liquid saturating a porous medium under the action of a vertical AC electric field and a vertical temperature gradient. In recent years, substantial research has been devoted to the stability analysis of viscoelastic fluids using Oldroyd, Kelvin-Voigt, and Maxwell models. For a more comprehensive overview of the subject, one may refer to Demir (2003), Kang et al. (2011), Bhadauria and Kiran (2014), Vadasz (2019), Raghunatha and Shivakumara (2021), Ibezim et al. (2021), and references cited therein. In the present time, the viscoelastic Navier–Stokes–Voigt fluid model, characterized by its mathematical simplicity and versatility, has become a focal point of interest among fluid dynamicists, with applications extending to organic polymer sciences, food engineering, and the biomechanical analysis of diffuse axonal injury. Oskolkov (1987) derived the differential and integro-differential equations governing the motion of the viscoelastic fluids. Oskolkov (1995) subsequently introduced a model for the Kelvin-Voigt fluid, which has been widely utilized to study the motion of fluids with very weak viscoelastic properties. Sukacheva and Matveeva (2010) considered a homogenous thermoconvection model of the non-compressible viscoelastic Kelvin–Voigt fluid of the non-zero order. Straughan (2021) investigated the thermosolutal convection with a Navier–Stokes–Voigt fluid and predicted that Kelvin–Voigt parameter has stabilizing effect for the oscillatory mode of convection. Straughan (2023) also presented a model for the study of the nonlinear stability for thermal convection with temperature dependent viscosity in a Navier–Stokes–Voigt fluid and showed that Kelvin–Voigt term plays an important role in stability analysis. For a more comprehensive understanding of the subject one may

* E-mail address: jpsmaths67@gmail.com
doi: 10.24352/UB.OVGU-2026-015
2026 | All rights reserved.

NOMENCLATURE

M	ratio of the heat capacities*	t	Time (T)
a^2	square of the wave number	V	root mean square value of electric potential ($ML^2T^{-3}I^{-1}$)
a_c	critical wave number (L^{-1})		
D	differential operator (L^{-1})	V_1	electric potential at upper surface ($ML^2T^{-3}I^{-1}$)
Da	Darcy number*	(u, v, w)	velocity components (LT^{-1})
d	thickness of the porous layer (L)	(x, y, z)	Cartesian co-ordinates (L)
$\vec{E}$	root mean square value of electric field ($MLT^{-3}I^{-1}$)		
$\vec{\Omega}$	Constant angular velocity	**Greek Symbols**	
$\vec{g}$	acceleration due to gravity (LT^{-2})	α	coefficient of volume expansion (Θ^{-1})
k	permeability of the porous medium (L^2)	ϵ	dielectric constant*
k_x	horizontal wave number along X-axis (L^{-1})	ϵ_0	reference dielectric constant*
k_y	horizontal wave number along Y-axis (L^{-1})	γ	thermal expansion coefficient of dielectric constant (Θ^{-1})
σ	complex growth rate (T^{-1})	κ	thermal diffusivity (L^2T^{-1})
σ_r	real part of complex growth rate (T^{-1})	Λ	ratio of viscosities*
σ_i	imaginary part of complex growth rate (T^{-1})	μ	fluid viscosity ($ML^{-1}T^{-1}$)
P	modified pressure ($ML^{-1}T^{-2}$)	$\tilde{\mu}$	effective viscosity ($ML^{-1}T^{-1}$)
Pr	Prandtl Number*	ν	kinematic viscosity (L^2T^{-1})
p	Pressure ($ML^{-1}T^{-2}$)	ρ_0	reference density (ML^{-3})
$\vec{q}$	Velocity (LT^{-1})	φ	porosity of the medium*
R_t	thermal Rayleigh number*	Φ	perturbation electric potential ($ML^2T^{-3}I^{-1}$)
R_i	Internal Rayleigh Number*	ρ	fluid density (ML^{-3})
R_{tc}	critical thermal Rayleigh number*	Θ	perturbation temperature (Θ^{-1})
R_{ea}	Electric Rayleigh number*	$\hat{\lambda}$	Navier-Stokes-Voigt parameter (L^2)
Ta	Taylor Number*		
R_{eac}	critical Electric Rayleigh number*	**Subscript**	
		b	Basic State
T	Temperature (Θ^{-1})	*	Non-dimensional quantity
T_0	temperature at the lower boundary (Θ^{-1})		
T_1	temperature at the upper boundary (Θ^{-1})		
Q	Heat generation within fluid layer		

refer to Matveeva (2013), Shankar and Shivakumara (2023), Badday and Harfash (2024), Kumari et al. (2024). Applications in geophysics and engineering serve as a driving force for the study of flow in rotating porous media. The food processing, chemical, and centrifugal filtration industries, as well as rotating machinery, are some of the engineering fields that use rotating flow in porous media. Gorla et al. (2011) examined the natural-convection-dominated regime of mixed convective boundary layer flow over a vertical wedge embedded in a nanofluid-saturated porous medium. Their analysis demonstrated the significant impact of thermal radiation and nanoparticle concentration on heat transfer enhancement along non-flat boundaries in porous domains. Alsabery et al. (2019) simulated free convection heat transfer inside a porous cavity filled with water-based nanofluid under the LTNE model, considering a cavity with an inner solid cylinder centered inside it and a heated, wavy bottom wall. Rasool et al. (2020) examined the flow of a Casson-type nanofluid through a porous medium over a non-linearly stretching surface using the Darcy–Forchheimer relation, incorporating slip boundary condition.

In a dielectric fluid, when a temperature gradient is applied in a dielectric fluid layer in the presence of some electric field, this results in some non-uniformities in the dielectric constant, amplifying the polarization force causing the fluid motion. The convection may manifest itself even if the temperature gradient stabilizes when the system is heated from above. The instability caused only by an electric field is called as electroconvection, whereas if the system is heated from below in the presence of an electric field, the resulting instability is known as electrothermoconvection (ETC) (Shivakumara et al., 2011). Understanding the effect of

internal heat generation is quite important in many applications, in fields such as metal waste, reactor safety analysis, spent nuclear fuel and strength of radioactive materials. In the case of a dielectric fluid, the applied electric field in the presence of a vertical temperature gradient enhances the vibrational motion of atoms, ultimately leading to heating throughout the fluid. As a result, it becomes more appropriate to account for uniform internal heat generation when analysing the onset of electrothermoconvection (ETC), since it modifies the fundamental temperature profile from linear to non-linear—significantly influencing ETC behaviour. Numerous studies have previously explored the impact of volumetric heat source distribution on the onset of thermal convection in viscous fluids and porous layers, given its relevance to convection phenomena in the Earth's mantle and its implications for thermal convection in cloud formations (Shivakumara et al., 2009). Analysis of such convection problems in the presence of an electric field helps in a better understanding of heat transfer processes since the fluid involved therein is dielectric and also in many technological problems, particularly in the design of more efficient heat exchangers. Chamkha and Issa (2000) studied the impact of heat absorption/generation and thermophoresis on convective flows. Shivakumara et al. (2007) investigated the combined effect of vertical DC electric field and uniform internal heat generation on the onset of convection in a horizontal poorly conducting dielectric fluid layer heated uniformly from below. Chamkha (2010) investigated double-diffusive convection in a porous enclosure under the combined influence of cooperating temperature and concentration gradients alongside heat generation or absorption effects. Yadav et al. (2017) investigated the criterion for the onset of convection induced by purely internal heating in a porous layer using Darcy Brinkman model. Shivaraj et al. (2021) studied the onset of Rayleigh–Bénard convection of variable viscosity in Newtonian dielectric liquid confined between two parallel plates subjected to free-free isothermal boundary condition. Kumari et al. (2024) examined the combined effect of an AC electric field and a vertical temperature gradient on a horizontal layer of viscoelastic dielectric fluid with internal heat source using Navier-Stokes-Voigt model. Recently, Reddy et al. (2025) examined the influence of internal heat and gravity modulation on the onset of double diffusive convection of Casson fluid using weakly non-linear analysis. In the present paper, the aim is to study the joint effect of vertical AC electric field, uniform rotation and internal heat source on the onset of Darcy-Brinkman convection in a Navier-Stokes-Voigt viscoelastic dielectric fluid with uniform internal heating saturating a porous layer either heated from below or above for free-free boundaries. It is pertinent to mention that although the effect of a vertical AC electric field on viscoelastic dielectric fluids, the role of internal heat generation in electrothermoconvection, and the influence of rotation on convective instability in porous media have each received attention independently, no study to date has examined the combined and simultaneous influence of an electric field, rotation and internal heat generation on a Navier–Stokes–Voigt viscoelastic dielectric fluid saturating a sparsely distributed (Darcy–Brinkman) porous medium. This gap forms the specific motivation and novelty of the present study. Furthermore, a real application of the coupled electric-field/rotation mechanism studied here is found in microgravity convection experiments, where a dielectric fluid subjected to a strong central electric field and rotation is used to emulate gravity-driven planetary convection aboard spacecraft—a technique realized in the ISS GeoFlow/AtmoFlow experiments and recently modelled by Gaillard et al. (2024). While that configuration does not include internal heating, viscoelasticity, or a porous medium, it confirms that electric-field-driven, rotation-modulated convection in a dielectric fluid is not merely of theoretical interest but is used in physical experimental design; the porous, viscoelastic and internally heated extensions considered in the present work are motivated by analogous requirements in engineered dielectric-fluid systems (e.g., insulation media, coolant matrices) where these additional physical effects cannot be neglected. The impact of electric field, rotation and the internal Rayleigh number on the fluid system for stationary convection and oscillatory convection is analysed numerically and predicted graphically by using the Mathematica software. Also, some of the known results are derived analytically as special cases. Furthermore, it is also predicted that the system is more stable when heated from above than heated from below. The results derived herein have not been reported yet in the literature to the best of authors' knowledge.

2 Mathematical Formulation of the Problem

2.1 When fluid layer is heated from below

Consider an infinite horizontal layer of Boussinesq dielectric Navier-Stokes-Voigt (NSV) viscoelastic fluid of finite vertical thickness d, saturating a sparsely distributed porous medium. The fluid layer is subjected to a uniform vertical AC electric field $\vec{E} = (0, 0, E)$, a vertical rotation with constant angular velocity $\vec{\Omega} = (0, 0, \Omega)$, and statically confined within the horizontal boundaries $z = 0$ and $z = d$, which are respectively maintained at uniform temperatures T_0 and T_1 $(< T_0)$ (see Fig. 1). It is assumed that the fluid and solid matrix are in local thermal equilibrium and rotation does not disrupt the isotropy of the porous medium (Shivakumara et al., 2011).

The basic equations, governing the flow of dielectric viscoelastic fluid (NSV Model), are given by (Shivakumara et al., 2011; Kumari et al., 2024)

$$\nabla \cdot \vec{q} = 0, \tag{1}$$

$$\rho_0 \left[\frac{1}{\varphi}(1 - \hat{\lambda}\nabla^2)\frac{\partial \vec{q}}{\partial t} + \frac{1}{\varphi^2}(\vec{q} \cdot \nabla)\vec{q} + \frac{2}{\varphi}(\vec{\Omega} \times \vec{q}) \right] = -\nabla P + \rho\vec{g} + \frac{\mu}{k}\vec{q} + \tilde{\mu}\nabla^2\vec{q} + \rho_e\vec{E} - \frac{1}{2}(\vec{E} \cdot \vec{E})\nabla\epsilon, \tag{2}$$

$$M\frac{\partial T}{\partial t} + (\vec{q} \cdot \nabla)T = \kappa\nabla^2 T + Q(T - T_1), \tag{3}$$

$$\rho = \rho_0[1 - \alpha(T - T_1)], \tag{4}$$

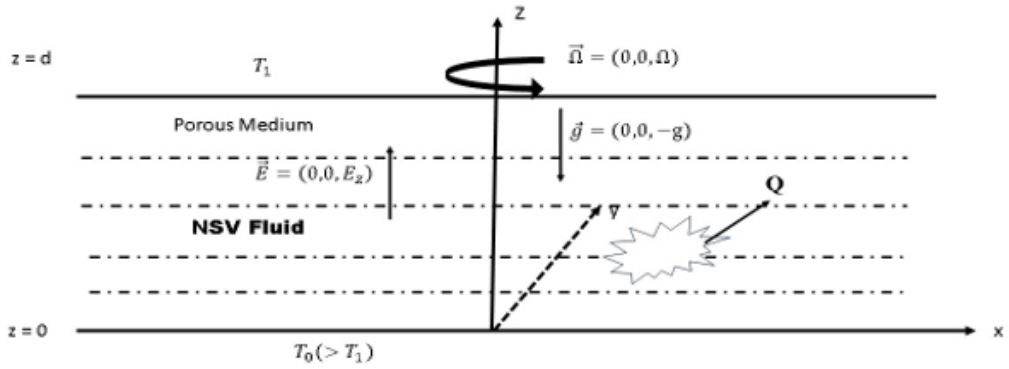


Fig. 1: Geometrical configuration of the problem.

where $\hat{\lambda}$ is the Navier-Stokes-Voigt coefficient, $\vec{q} = (u, v, w)$ is the velocity vector, $P = p - \frac{1}{2}\rho\frac{\partial\epsilon}{\partial\rho}(\vec{E}\cdot\vec{E})$ is the modified pressure, ρ is the fluid density, κ is the effective thermal diffusivity, k is the permeability of the porous medium, μ is the fluid viscosity, $\tilde{\mu}$ is the effective viscosity, $\vec{g} = (0, 0, -g)$ is the acceleration due to gravity, φ is the porosity of the porous medium, $M = (\rho_0 c)_m/(\rho_0 c_p)_f = [(1-\varphi)(\rho_0 c)_m + \varphi(\rho_0 c_p)_f]/(\rho_0 c_p)_f$ is the ratio of heat capacities of the fluid saturating porous medium to that of the fluid, c is the specific heat, c_p is the specific heat at constant pressure, α is the thermal expansion coefficient, ρ_0 is the reference value of fluid density, T is the temperature, T_1 is the temperature at upper plate, Q is uniformly distributed volumetric heat generation within the fluid layer. Further, a positive value of Q will give rise to an increase in the temperature of the layer and therefore is an internal heat source. Thus, a negative value of Q represents an internal heat sink. In the above equations, $\vec{E} = (0, 0, E)$ is the root mean square value of the electric field, ρ_e is the free charge density, and ϵ is the dielectric constant. In the right-hand side of Eq. (2) fourth term, $\rho_e\vec{E}$ (Coulomb force) due to smallness, can be neglected in comparison to the fifth term, $\frac{1}{2}(\vec{E}\cdot\vec{E})\nabla\epsilon$ (Dielectrophoretic force) (Takashima, 1976). Thus Eq. (2) modifies to

$$\rho_0\left[\frac{1}{\varphi}(1-\hat{\lambda}\nabla^2)\frac{\partial\vec{q}}{\partial t} + \frac{1}{\varphi^2}(\vec{q}\cdot\nabla)\vec{q} + \frac{2}{\varphi}(\vec{\Omega}\times\vec{q})\right] = -\nabla P + \rho\vec{g} + \frac{\mu}{k}\vec{q} + \tilde{\mu}\nabla^2\vec{q} - \frac{1}{2}(\vec{E}\cdot\vec{E})\nabla\epsilon. \tag{5}$$

The Maxwell's equations pertinent to the current context are

$$\nabla\times\vec{E} = 0, \tag{6}$$

$$\nabla\cdot(\epsilon\vec{E}) = 0. \tag{7}$$

In the light of Eq. (6), $\vec{E}$ can be expressed as

$$\vec{E} = \nabla V, \tag{8}$$

where V is the root mean square value of the electric potential. The dielectric constant given by

$$\epsilon = \epsilon_0[1-\gamma(T-T_1)], \tag{9}$$

where ϵ_0 is the value of the dielectric constant and γ ($\gamma > 0$) is the thermal expansion coefficient of the dielectric constant and is considered to be small (Maekawa, 1992).
The basic state is considered to be stationary and is given by

$$\begin{aligned}&\vec{q} = (0,0,0), \quad T = T_b(z), \quad \vec{E} = \vec{E}_b, \quad \epsilon = \epsilon_b(z),\\ &T_b = T_1 + \Delta T\, G(z), \quad \epsilon = \epsilon_0(1-\gamma\Delta T\, G(z)), \quad \rho_b = \rho_0(1-\alpha\Delta T\, G(z)),\end{aligned} \tag{10}$$

where, the subscript b denotes the basic state and

$$G(z) = \frac{\sin\left(\sqrt{R_i}\left(1-\frac{z}{d}\right)\right)}{\sin\sqrt{R_i}},$$

where, $R_i = \frac{Qd^2}{\kappa}$ is known as internal Rayleigh number. In the view of Eq. (7) and $E_{bx} = E_{by} = 0$, it follows that

$$\epsilon_b E_{bz} = \epsilon_0 E_0 = \text{constant (say)}, \tag{11}$$

which on utilizing (10), yields

$$E_{bz} = \frac{E_0}{1-\gamma\Delta T\, G(z)} = E_b(z). \tag{12}$$

To examine the stability of the initial state, we introduce infinitesimally small perturbations $(\vec{q}', P', \vec{E}', T', \rho', \epsilon')$ on the basic state in the form

$$\vec{q} = \vec{q}', \quad P = P_b + P', \quad \vec{E} = \vec{E}_b + \vec{E}', \quad T = T_b + T', \quad \rho = \rho_b + \rho', \quad \epsilon = \epsilon_b + \epsilon'. \tag{13}$$

Now, substituting Eq. (13) in Eqs. (1)–(8), utilizing the basic state solutions, we obtain the perturbation equations which are linearized by omitting the product of perturbations. These perturbation equations are further simplified by eliminating the pressure term by applying curl twice to obtain the following set of equations (after neglecting the primes for simplicity),

$$\left(\frac{1}{\varphi}(1-\hat{\lambda}\nabla^2)\frac{\partial}{\partial t} + \frac{\mu}{\rho_0 k} - \frac{\tilde{\mu}}{\rho_0}\nabla^2\right)\nabla^2 w = \alpha g \nabla_h^2 T - \frac{2\Omega}{\varphi}\frac{\partial \zeta}{\partial z} - \nabla_h^2\left[\frac{E_0\epsilon_0\gamma\Delta T\, G'(z)}{\rho_0}\left(\gamma E_0 T + \frac{\partial V}{\partial z}\right)\right], \tag{14}$$

$$\left(\frac{1}{\varphi}(1-\hat{\lambda}\nabla^2)\frac{\partial}{\partial t} + \frac{\mu}{\rho_0 k} - \frac{\tilde{\mu}}{\rho_0}\nabla^2\right)\zeta = \frac{2\Omega}{\varphi}\frac{\partial w}{\partial z}, \tag{15}$$

$$\left(M\frac{\partial}{\partial t} - Q - \kappa\nabla^2\right)T = -w\, g_2(z), \tag{16}$$

$$\nabla^2 V = -\gamma E_0 \frac{\partial T}{\partial z}, \tag{17}$$

where $\nabla_h^2 = \frac{\partial^2}{\partial x^2} + \frac{\partial^2}{\partial y^2}$ and $\zeta = \frac{\partial v}{\partial x} - \frac{\partial u}{\partial y}$ are horizontal Laplacian operator and vertical component of perturbation vorticity respectively. Now, non-dimensionalizing Eqs. (14)–(17), by scaling (x, y, z) by d, t by $\frac{d^2}{\kappa}$, w by $\frac{\kappa}{d}$, ζ by $\frac{\kappa}{d^2}$, T by ΔT, $\hat{\lambda}$ by $\frac{1}{t\kappa}$ and V by $\gamma E_0 \Delta T d$, we obtain

$$\left(\frac{1}{Pr}(1-\hat{\lambda}\nabla^2)\frac{\partial}{\partial t} - \Lambda\nabla^2 + Da^{-1}\right)\nabla^2 w = R_t \nabla_h^2 T - Ta^{\frac{1}{2}}\frac{\partial \zeta}{\partial z} - G'(z) R_{ea}\nabla_h^2\left(T + \frac{\partial V}{\partial z}\right), \tag{18}$$

$$\left(\frac{1}{Pr}(1-\hat{\lambda}\nabla^2)\frac{\partial}{\partial t} - \Lambda\nabla^2 + Da^{-1}\right)\zeta = Ta^{\frac{1}{2}}\frac{\partial w}{\partial z}, \tag{19}$$

$$\left(M\frac{\partial}{\partial t} - R_i - \nabla^2\right)T = -w\, g_2(z), \tag{20}$$

$$\nabla^2 V = -\frac{\partial T}{\partial z}, \tag{21}$$

where, $R_t = \alpha g \beta d^4/\nu\kappa$ is the thermal Rayleigh number, $R_{ea} = \gamma^2\epsilon_0 E_0^2\beta^2 d^4/\mu\kappa$ is the AC electric Rayleigh number, $Da = k/d^2$ is the Darcy number, $Ta = 4\Omega^2 d^4/\nu^2\varphi^2$ is the modified Taylor number, $Pr = \nu\varphi/\kappa$ is the modified Prandtl number, $\Lambda = \tilde{\mu}/\mu$ is the ratio of the viscosities and

$$g_2(z) = \frac{\mathrm{d}T_b}{\mathrm{d}z} = -\sqrt{R_i}\,\frac{\cos\left(\sqrt{R_i}(1-z)\right)}{\sin\sqrt{R_i}}.$$

Now, to carry out the linear stability analysis, we use the normal mode technique describing the perturbation a dependence on and of the form

$$(w, T, V, \zeta)(x, y, z, t) = (W(z), \Theta(z), \Phi(z), Z(z))\exp[i(k_x x + k_y y) + \sigma t], \tag{22}$$

where k_x and k_y are the wave numbers along x and y directions respectively, and σ $(= \sigma_r + i\sigma_i)$ is the complex growth rate. On substituting Eq. (22) in Eqs. (18)–(21), we obtain the governing equations in non-dimensional form as

$$\left(\frac{\sigma(1-\hat{\lambda}(D^2-a^2))}{Pr} - \Lambda(D^2-a^2) + Da^{-1}\right)(D^2-a^2)W = -R_t a^2\Theta - Ta^{\frac{1}{2}}DZ + R_{ea}a^2 DG(z)\,(\Theta + D\Phi), \tag{23}$$

$$\left(\frac{\sigma(1-\hat{\lambda}(D^2-a^2))}{Pr} - \Lambda(D^2-a^2) + Da^{-1}\right)Z = Ta^{\frac{1}{2}}DW, \tag{24}$$

$$(D^2 - a^2 + R_i - M\sigma)\Theta = W g_2(z), \tag{25}$$

$$(D^2 - a^2)\Phi = -D\Theta, \tag{26}$$

together with the boundary conditions

$$W = D^2 W = \Theta = D\Phi = DZ = 0 \quad \text{for a free boundary,} \tag{27}$$

and

$$W = DW = \Theta = \Phi = Z = 0 \quad \text{for a rigid boundary,} \tag{28}$$

where $D = \frac{\mathrm{d}}{\mathrm{d}z}$ is the differentiation with respect to vertical coordinate z, $a^2 = k_x^2 + k_y^2$ is square of the resultant wave number, W is z-component of the perturbation velocity, Θ is the perturbation temperature, Φ is the perturbation electrical potential and Z is z-component of the perturbation vorticity.

3 Linear Stability Analysis

3.1 When fluid is heated from below

The exact solution of the eigenvalue problem is obtained for free-free boundaries. In order to satisfy boundary conditions (27) on both the boundaries, we assume the solution for W, Θ, Φ and Z of the form

$$W = C_1 \sin \pi z, \quad \Theta = C_2 \sin \pi z, \quad \Phi = C_3 \cos \pi z, \quad Z = C_4 \cos \pi z, \tag{29}$$

where C_1, C_2, C_3, C_4 are constants. Substituting Eq. (29) into Eqs. (23)–(26), multiplying the resulting equations by $\sin \pi z$ and integrating each equations from $z = 0$ and $z = 1$ and we can derive the condition for the existence of a non-trivial eigenvalue as

$$\begin{vmatrix} \left(\frac{\sigma\xi}{Pr} + \eta\delta^2\right)\delta^2 & -a^2(R_t - 2FR_{ea}) & -2\pi a^2 F R_{ea} & \pi T a^{1/2} \\ -\pi T a^{1/2} & 0 & 0 & \left(\frac{\sigma\xi}{Pr} + \eta\delta^2\right) \\ 2F & (M\sigma + \delta^2 - R_i) & 0 & 0 \\ 0 & -\pi & \delta^2 & 0 \end{vmatrix} = 0, \tag{30}$$

where $\eta = \left(\Lambda + \frac{Da^{-1}}{\delta^2}\right)$, $\xi = (1 + \hat{\lambda}\delta^2)$, $\delta^2 = \pi^2 + a^2$ and $F = \int_0^1 g_2(z) \sin^2 \pi z \, \mathrm{d}z = -\frac{2\pi^2}{4\pi^2 - R_i}$, respectively. On expanding (30) yields the following cubic dispersion relation,

$$\sigma^3 + \alpha_1 \sigma^2 + \alpha_2 \sigma + \alpha_3 = 0, \tag{31}$$

where,

$$\alpha_1 = \delta^2 \left(\frac{1}{M} + \frac{2Pr\,\eta}{\xi} - \frac{R_i}{M\delta^2}\right), \tag{32}$$

$$\alpha_2 = \frac{a^2 Pr}{\delta^2}\left(\frac{\delta^6\eta^2 Pr}{a^2\xi^2} + \frac{2\delta^6\eta}{Ma^2\xi} + \frac{\pi^2 Pr\, Ta}{a^2\xi^2} + \frac{2FR_t}{M\xi} - \frac{4a^2F^2R_{ea}}{M\xi\delta^2} - \frac{2\delta^4\eta R_i}{Ma^2\xi}\right), \tag{33}$$

$$\alpha_3 = a^2\eta Pr^2\left(\frac{\delta^6\eta}{Ma^2\xi^2} + \frac{\pi^2 Ta}{M\xi^2 a^2\eta} - \frac{\pi^2 Ta R_i}{M\xi^2 a^2\eta\delta^2} + \frac{2FR_t}{M\xi^2} - \frac{4a^2F^2R_{ea}}{M\xi^2\delta^2} - \frac{\delta^4\eta R_i}{Ma^2\xi^2}\right). \tag{34}$$

Thus, putting $\sigma = 0$ in Eq. (31), yields expression for Rayleigh number for stationary convection, defined by $R_t = R_t^s$, where,

$$R_t^s = \left(\frac{-1}{2F}\right)\left(\frac{\eta\delta^6}{a^2} + \frac{\pi^2 Ta}{a^2\eta} - \frac{4a^2F^2R_{ea}}{\delta^2} - \frac{\pi^2 Ta R_i}{a^2\eta\delta^2} - \frac{\eta\delta^4 R_i}{a^2}\right). \tag{35}$$

Thus, in the absence of internal heat source i.e. $R_i = 0$ and $F = -\frac{1}{2}$ we have the thermal Rayleigh number, as a function of the parameter $R_{ea}, a, \sigma, \hat{\lambda}, Pr, \Lambda, Da^{-1}$ and Ta.

$$R_t^s = \frac{\eta\delta^6}{a^2} + \frac{\pi^2 Ta}{a^2\eta} - \frac{a^2}{\delta^2}R_{ea}, \tag{36}$$

which expresses Rayleigh number for stationary convection for electrothermoconvection in a rotating Brinkman porous medium (Shivakumara et al., 2011). When $Da^{-1} \to 0$, $\Lambda = 1$ and $Ta = 0$, Eq. (35) reduces to,

$$R_t^s = -\frac{\delta^4}{2Fa^2}(\delta^2 - R_i) + \frac{2Fa^2}{\delta^2}R_{ea}, \tag{37}$$

which is result obtained by Kumari et al. (2024) for Electrothermoconvection in the presence of Internal Heat source.
Under some limiting cases, Eq. (36) provides some existing results in the literature. In the absence of an electric field (i.e., $R_{ea} = 0$) and rotation (i.e., $Ta = 0$), the above equation reduces to

$$R_t^s = \frac{\delta^4(\Lambda\delta^2 + Da^{-1})}{a^2}, \tag{38}$$

which is the expression for Rayleigh number for stationary convection in Brinkman porous medium. If we set $Da^{-1} \to 0$ and $\Lambda = 1$, in Eq. (37), we have

$$R_t^s = \frac{(\pi^2 + a^2)^3}{a^2}, \tag{39}$$

a result derived by Chandrasekhar (1981) for the ordinary viscous fluid. When $Ta = 0$, $\Lambda = 1$ and $Da^{-1} \to 0$, Eq. (36) reduces to

$$R_t^s = \frac{\delta^6}{a^2} - \frac{a^2}{\delta^2}R_{ea}, \tag{40}$$

which is in good agreement with Roberts (1969). To find the critical value of R_t^s, Eq. (35) is differentiated with respect to a^2 and equated to zero, which gives

$$\frac{1}{4}\left(\begin{array}{l} 4Da^{-1} + 2a^2\Lambda\left(4 - \dfrac{R_i}{\pi^2}\right) - \dfrac{R_i Da^{-1}}{\pi^2} - \dfrac{16\pi^4 R_{ea}}{(a^2+\pi^2)^2(-R_i + 4\pi^2)} - \dfrac{2\Lambda(R_i^2 - 5R_i\pi^2 + 4\pi^4)Ta}{a^2(Da^{-1} + \Lambda(a^2+\pi^2))^2} \\ - \dfrac{(Da^{-1} + \Lambda\pi^2)(R_i^2 - 5R_i\pi^2 + 4\pi^4)Ta}{a^4(Da^{-1} + \Lambda(a^2+\pi^2))^2} + \Lambda\left(-7R_i + \dfrac{R_i^2}{\pi^2} + 12\pi^2 + \dfrac{(R_i - 4\pi^2)Ta}{(Da^{-1} + \Lambda(a^2+\pi^2))^2}\right) \end{array}\right) = 0. \tag{41}$$

The above equation is solved numerically for various values of R_{ea}, Λ, Ta and Da^{-1}, and minimum value of a_c^2 obtained each time, hence the critical wave number is obtained.
To analyse the onset of oscillatory convection, we substitute $\sigma = i\sigma_i$ in Eq. (31) and equating the real and imaginary parts of the corresponding equation to obtain

$$\sigma_i^2 = \frac{\alpha_3}{\alpha_1} \quad \text{and} \quad \sigma_i^2 = \alpha_2. \tag{42}$$

Eliminating σ_i finally leads to an expression for Rayleigh's number $R_t = R_t^o$ at which the oscillatory convection occurs, where,

$$\begin{aligned} R_t^o = & -\frac{\eta\delta^2(\xi + Pr\,\eta M)^2}{a^2\xi F(Pr\,\eta M\delta^2 + \xi\delta^2 - \xi R_i)}\left(\delta^6 + \pi^2 Ta\left(\frac{PrM}{\xi + Pr\,\eta M}\right)^2\right) \\ & + \frac{\eta\delta^4 R_i}{a^2 F}\left(2 + \frac{\xi R_i}{Pr\,\eta M\delta^2 + \xi\delta^2 - \xi R_i}\right) + \frac{2a^2 F R_{ea}}{\delta^2}. \end{aligned} \tag{43}$$

Thus, in the absence of internal heat source i.e. $R_i = 0$ and $F = -\frac{1}{2}$, we derive the oscillatory thermal Rayleigh number; given by

$$R_t^o = \frac{2\eta}{a^2\xi}(\xi + Pr\,\eta M)\left(\delta^6 + \pi^2 Ta\left(\frac{PrM}{\xi + Pr\,\eta M}\right)^2\right) - \frac{a^2 R_{ea}}{\delta^2}, \tag{44}$$

which is the expression for thermal Rayleigh number for oscillatory convection in NSV rotating Brinkman porous medium (Singh et al., 2025). Now from Eq. (41), it is clear that oscillatory instability (for $\sigma_i^2 > 0$) can occur only if either of two cases arises:

$$\begin{aligned} &\text{Case 1: } \delta^2 > R_i, \text{ then } 0 < Pr < \frac{\xi(\delta^2 - R_i)}{M\eta\delta^2}, \\ &\qquad \text{and } Ta > \frac{\eta^2\delta^6}{\pi^2}\left(\frac{\xi(\delta^2 - R_i) + Pr\,\eta M\delta^2}{\xi(\delta^2 - R_i) - Pr\,\eta M\delta^2}\right). \end{aligned} \tag{45}$$

$$\begin{aligned} &\text{Case 2: } \delta^2 < R_i, \text{ then } 0 < Pr < \frac{\xi(R_i - \delta^2)}{M\eta\delta^2}, \\ &\qquad \text{and } Ta > \frac{\eta^2\delta^6}{\pi^2}\left(\frac{\xi(R_i - \delta^2) - Pr\,\eta M\delta^2}{\xi(R_i - \delta^2) + Pr\,\eta M\delta^2}\right). \end{aligned} \tag{46}$$

In the absence of internal heat source i.e. $R_i = 0$ and $F = -\frac{1}{2}$, above two cases reduce to a single expression given as

$$0 < Pr < \frac{\xi}{M\eta}, \quad \text{and} \quad Ta > \frac{\eta^2\delta^6}{\pi^2}\left(\frac{\xi + Pr\,\eta M}{\xi - Pr\,\eta M}\right) \tag{47}$$

which is the condition for the manifestation of oscillatory convection in NSV fluid saturating a rotating Brinkman porous medium (Singh et al., 2025).
It is interesting to note that when we consider the Navier-Stokes-Voigt parameter $\hat{\lambda} = 0$ we get $\xi = 1$, then Eqs. (43) and (46) will become

$$R_t^o = \frac{2\eta}{a^2}(1 + Pr\,\eta M)\left(\delta^6 + \pi^2 Ta\left(\frac{PrM}{1 + Pr\,\eta M}\right)^2\right) - \frac{a^2 R_{ea}}{\delta^2} \tag{48}$$

$$0 < Pr < \frac{1}{M\eta} \quad \text{and} \quad Ta > \frac{\eta^2\delta^6}{\pi^2}\left(\frac{1 + Pr\,\eta M}{1 - Pr\,\eta M}\right) \tag{49}$$

A result due to Shivakumara et al. (2011) obtained for electrothermoconvection in a rotating Brinkman porous layer. For the non-porous medium (i.e., $Da^{-1} \to 0$, $\Lambda = 1$, and $M = 1 = \varphi$), the Eq. (48) gives

$$Pr < 1 \quad \text{and} \quad Ta > \frac{\delta^6}{\pi^2}\left(\frac{1 + Pr}{1 - Pr}\right) \tag{50}$$

which coincides with Chandrasekhar (1981).

3.2 When fluid is heated from above

For the case when fluid layer is heated from above, then we have $R_t < 0$. Therefore, substituting $R_t = -|R_t|$ in Eq. (23), and following the same procedure as used to derive the Eqs. (35) and (41), the expression for thermal Rayleigh number for stationary and oscillatory convection are, respectively,

$$\left|R_t^s\right| = \frac{1}{2F}\left(\frac{\eta\delta^6}{a^2} + \frac{\pi^2 Ta}{a^2\eta} - \frac{4a^2F^2R_{ea}}{\delta^2} - \frac{\pi^2 TaR_i}{a^2\eta\delta^2} - \frac{\eta\delta^4 R_i}{a^2}\right), \tag{51}$$

and

$$\begin{aligned}\left|R_t^o\right| = {} & \frac{\eta\delta^2\,(\xi + Pr\,\eta M)^2}{a^2\xi F\left(Pr\,\eta M\delta^2 + \xi\delta^2 - \xi R_i\right)}\left(\delta^6 + \pi^2 Ta\left(\frac{PrM}{\xi + Pr\,\eta M}\right)^2\right) \\ & - \frac{\eta\delta^4 R_i}{a^2F}\left(2 + \frac{\xi R_i}{Pr\,\eta M\delta^2 + \xi\delta^2 - \xi R_i}\right) - \frac{2a^2FR_{ea}}{\delta^2}.\end{aligned} \tag{52}$$

4 Results and Discussions

In the present study, we have used linear stability theory to examine the effects of vertical AC electric field, uniform rotation and internal heat source on the onset of convection in a Navier Stokes Voigt viscoelastic dielectric fluid saturating a porous layer heated from below and above separately using Darcy-Brinkman model for free-free boundaries. The eigenvalue problem is solved exactly in the case of free-free boundaries. We validate the numerical results, by comparing critical Rayleigh number R_{tc} and the corresponding wave number a_c obtained for different values of R_i and Λ when $Da^{-1} = 0.01$, $R_{ea} = 0$, and $Ta = 10$ with those of Odok et al. (2020) in Table 1 and Table 2, respectively. The comparisons show significant agreement. Further, the variation of critical Rayleigh number R_{tc} and the corresponding wave number a_c obtained for different values of R_{ea} and Ta when $Da^{-1} = 0.01$, $R_i = 0.5$, and Λ, is shown the Table 3 and Table 4 respectively, which clearly predicts that increasing electric Rayleigh number R_{ea} has a destabilizing effect, while increasing Taylor number Ta has a stabilizing effect on the stationary convection.
Numerical studies have been performed using the Mathematica software. We studied the effects of various parameters, such as inverse Darcy number Da^{-1}, ratio of viscosities Λ, electric Rayleigh number R_{ea}, Taylor number Ta, internal Rayleigh number R_i and NSV parameters $\hat{\lambda}$ on the stability of the system; and the results are depicted through graphs for free boundaries. Fig. 2(a), Fig. 3(a), Fig. 4(a), Fig. 5(a) and Fig. 6(a) represent studies for stationary convection while Fig. 2(b), Fig. 3(b), Fig. 4(b), Fig. 5(b), Fig. 6(b) and Fig. 7 represent studies for the oscillatory mode of convection when the system is heated from below. Fig. 8 and Fig. 9 represent studies for both oscillatory and stationary modes of convection when the system is heated from below and above. Moreover, Fig. 10(a) and Fig. 11 illustrate the studies for stationary mode of convection and Fig. 10(b) illustrate study for the oscillatory mode of convection when the system is heated from above. Further, in plotting figures except for the one parameter, being varied, the values of the other parameters are held constant as $R_i = 5$, $R_{ea} = 100$, $Da^{-1} = 100$, $Pr = 5$, $\hat{\lambda} = 0.1$, $\Lambda = 1$ and $Ta = 10$.
Fig. 2(a) and Fig. 2(b) predict the variation of the thermal Rayleigh number with wave number for stationary and oscillatory convection respectively, when the values the internal Rayleigh number are considered as $R_i = 0, 1, 3$ and 5. From these graphs, it

Tab. 1: Comparison of critical Rayleigh number R^s_{tc}, and corresponding wave number a_c, for different values of R_t with $Da^{-1} = 0.01$ when $R_{ea} = 0$, $\lambda = 10$ and $Ta = 10$.

R_i	Odok et al. (2020)		Present Paper	
	a_c	R^s_{tc}	a_c	R^s_{tc}
0	2.2220	6577.53	2.2220	6577.56
0.5	2.2027	6274.29	2.2027	6274.32
1	2.1823	5975.36	2.1823	5975.38
1.5	2.1607	5680.64	2.1607	5680.66
2	2.1377	5390.06	2.1377	5390.08
2.5	2.1132	5103.48	2.1132	5103.50
3	2.0869	4820.78	2.0869	4820.80
3.5	2.0586	4541.79	2.0586	4541.81
4	2.0281	4266.30	2.0281	4266.32
4.5	1.9949	3994.07	1.99485	3994.09
5	1.9585	3724.78	1.9585	3724.80

Tab. 2: Comparison of critical Rayleigh number R^s_{tc}, and corresponding wave number a_c, for different values of Λ with $R_i = 0.5$, $Da^{-1} = 0.01$, $R_{ea} = 0$ and $Ta = 10$.

Λ	Odok et al. (2020)		Present Paper	
	a_c	R^e_c	a_c	R^e_c
1	2.2510	646.59	2.2509	646.595
2	2.2148	1264.46	2.2148	1264.46
3	2.2079	1888.46	2.2078	1888.46
4	2.2054	2514.04	2.2054	2514.05
5	2.2043	3140.27	2.20426	3140.28
6	2.3036	3766.82	2.3036	3766.83
7	2.2033	4393.55	2.20325	4393.56
8	2.2030	5020.39	2.2030	5020.41
9	2.2028	5647.32	2.2028	5647.34
10	2.2027	6274.29	2.2027	6274.32

can be seen that with an increase in the internal Rayleigh number there is a corresponding decrease in the critical thermal Rayleigh number which implies that the presence of an internal heat source is found to induce a destabilizing effect on both stationary and oscillatory convection. This is due to the fact that the internal heat source has the tendency to increase the energy supply of the hydrodynamic system. Fig. 3(a) and Fig. 3(b), respectively, illustrate the dependence of the thermal Rayleigh number on the different values of Λ, specifically at $\Lambda = 1, 4$ and 8. As pointed out by many researchers (Vadasz, 2019), Brinkman's model rests on an effective viscosity $\tilde{\mu}$ different from fluid viscosity μ denoted through Λ in dimensionless form, it has a determining influence on the onset of electrothermal convection in porous media.

We can see from the figures that ratio of viscosities Λ has stabilizing effect on the system in both mode of convection as an increase in Λ leads to strengthening of the viscous effect, which in turn resists the fluid flow. Further, Fig. 4(a) and Fig. 4(b) predict the variation of the thermal Rayleigh number with wave number for different values of Da^{-1}, specifically at $Da^{-1} = 0, 10$ and 100. It is evident from the figures that increasing the inverse Darcy number has stabilizing effects on both modes of convection. This occurs because an increase in Da^{-1} reduces the permeability of the porous medium, which in turn delays the instability. Fig. 5(a) and Fig. 5(b), illustrate the dependence of the thermal Rayleigh number on the Taylor number Ta, specifically at $Ta = 0, 500$ and 1000 for both modes of convection respectively. It is evident from the figures that increasing the Taylor number has stabilizing effects on both modes of convection. Fig. 6(a) and Fig. 6(b) predict the variation of the thermal Rayleigh number with wave number for stationary and oscillatory convection when the values of the electric Rayleigh number are considered as $R_{ea} = 0, 1000$ and 2000. From these graphs, it can be seen that with an increase in the electric Rayleigh number R_{ea}, there is a corresponding decrease in

Tab. 3: The variation of critical Rayleigh number R^s_{tc}, and corresponding wave number a_c, for different values of R_{ea} with $Da^{-1} = 0.01$ when $R_i = 0.5$, $\Lambda = 10$ and $Ta = 10$.

R_m	Present Paper	
	a_c	R^e_c
0	2.2027	6274.32
100	2.2086	6240.87
200	2.2145	6207.31
300	2.2205	6173.63
400	2.2264	6139.83
500	2.2325	6105.91
600	2.2385	6071.86
700	2.2446	6037.69
800	2.2506	6003.40
1000	2.2629	5934.45

Tab. 4: The variation of critical Rayleigh number R^s_{tc}, and corresponding wave number a_c, for different values of Ta with $Da^{-1} = 0.01$ when $R_i = 0.5$, $\Lambda = 10$ and $R_{ea} = 100$.

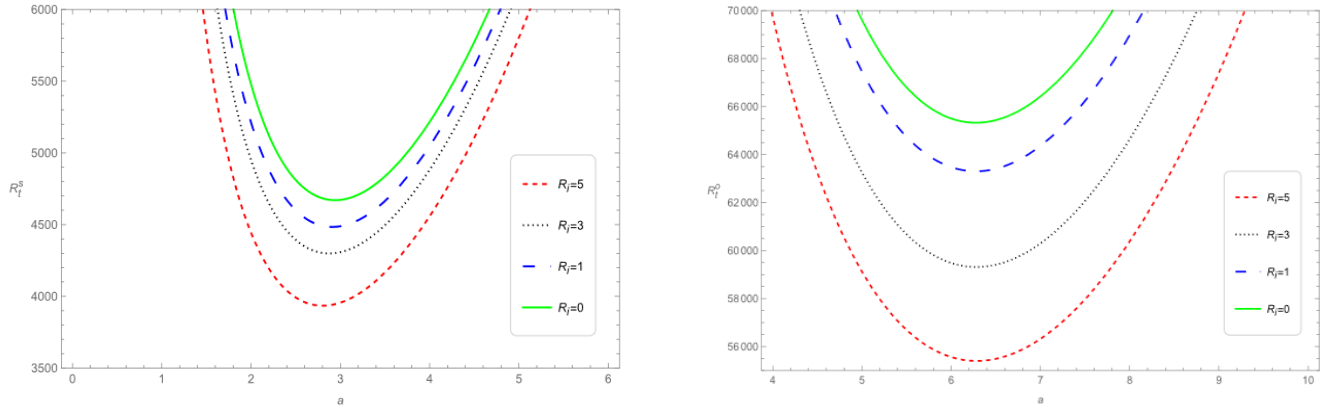
Ta	Present Paper	
	a_c	R^e_c
0	2.2081	6238.94
10	2.2086	6240.87
100	2.2131	6277.39
200	2.2181	6315.49
400	2.2279	6353.26
600	2.2376	6390.72
800	2.2471	6427.87
1000	2.2565	6609.23
2000	2.3014	6609.23
5000	2.41947	7116.43

the critical thermal Rayleigh number which implies that the presence of an AC electric field is to induce a destabilizing effect on both modes of convection because a strong electric field promotes more efficient transfer of heat energy through the fluid. Fig. 7 shows the variation of the oscillatory thermal Rayleigh number with wave number for different values of the NSV parameter $\hat{\lambda}$, specifically at $\hat{\lambda} = 0.1, 0.2$ and 0.3 (Kumar et al., 2025; Priyanshu and Deepika, 2026). This illustration suggests that as the NSV parameter $\hat{\lambda}$ increases, there is an observed decrease in the critical oscillatory thermal Rayleigh number, indicating that the NSV parameter exerts a destabilizing influence on oscillatory convection. This is due to the reason that elastic energy storage increases the disturbances and thus foster the instability.

Fig. 8 illustrate that the critical wave number a_c increases slowly with in both mode of convection. Thus, in this case, the size of convection cells is reduced as the value of R_{ea} increase. Fig. 9 also depicts that the critical wave number a_c increases with increasing Ta and hence resulting into the reduction in the size of the convection cells.

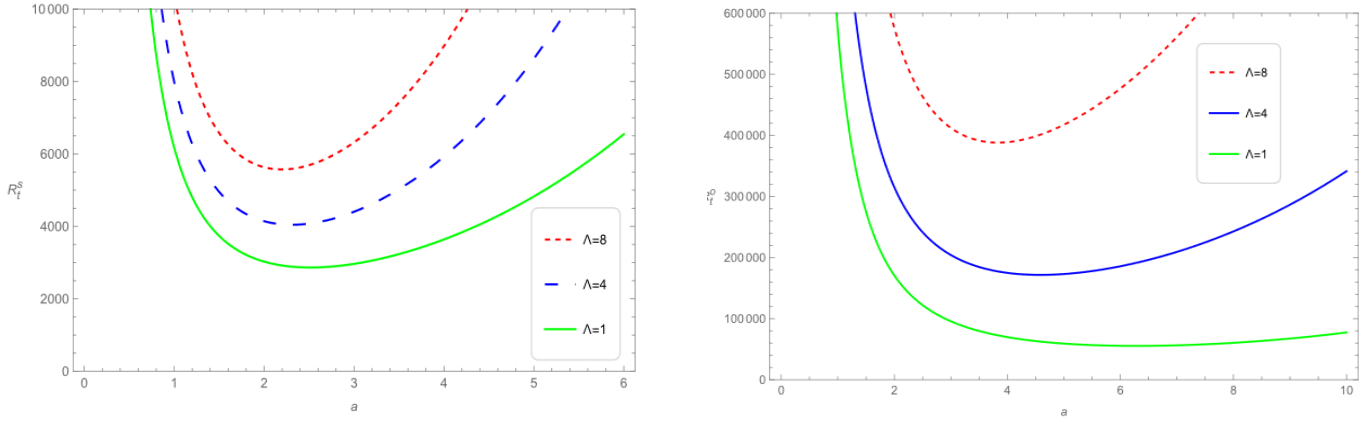
The Fig. 10(a) represents the marginal stability curves in (R_{ea}, a)-plane for the cases when the system is heated from above ($R_t = -500$), when the system is heated from below ($R_t = 500$) and when there is no heat ($R_t = 0$) supplied to the system (i.e. when instability occur due to AC electric field only) for stationary mode of convection. Similarly, the oscillatory mode of convection in (R_{ea}, a)-plane is discussed in Fig. 10(b) for all these cases of R_t. In both stationary as well as oscillatory modes the system heated from above is more stable compared to when there is no heat supplied to the system which in turn is more stable than when heated from below. The reason for this is that heating from above tends to make system bottom-heavy, thus imparting stabilizing effect on the system and instability arises only due to AC electric field applied.

The Fig. 11 represents the lines in (a, Ta)-plane for two values of $R_t = -500$ (heated from above) and $R_t = 500$ (heated from



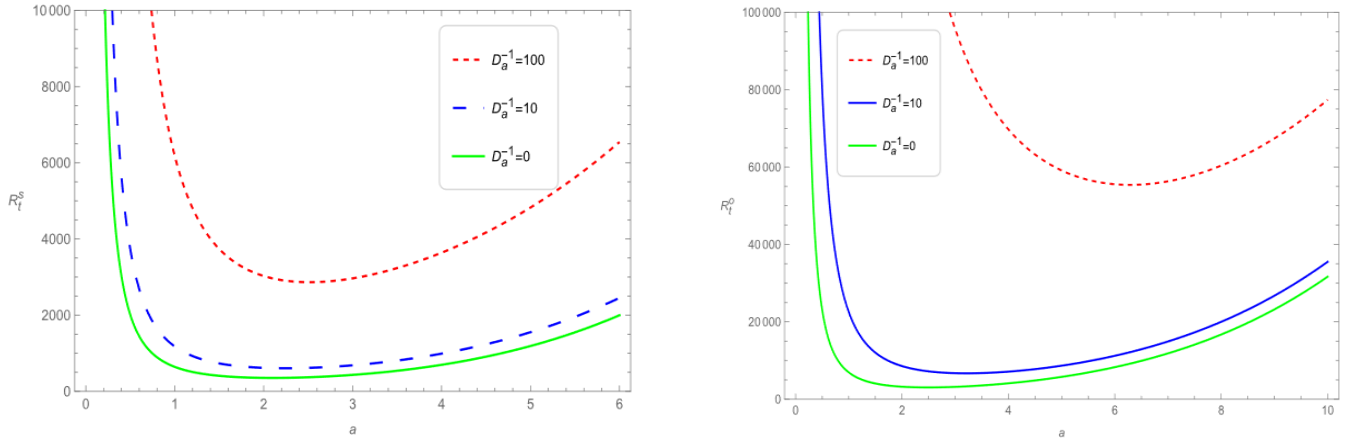
(a) (b)

Fig. 2: (a) R_t^s vs a for various values of R_i with $R_{ea} = 100$, $Da^{-1} = 100$, $\Lambda = 1$ and $Ta = 10$ (for Stationary Convection); (b) R_t^o vs a for various values of R_i with $R_{ea} = 100$, $Da^{-1} = 100$, $Pr = 5$, $\hat{\lambda} = 0.1$, $M = 1$, $\Lambda = 1$ and $Ta = 10$ (for oscillatory Convection).



(a) (b)

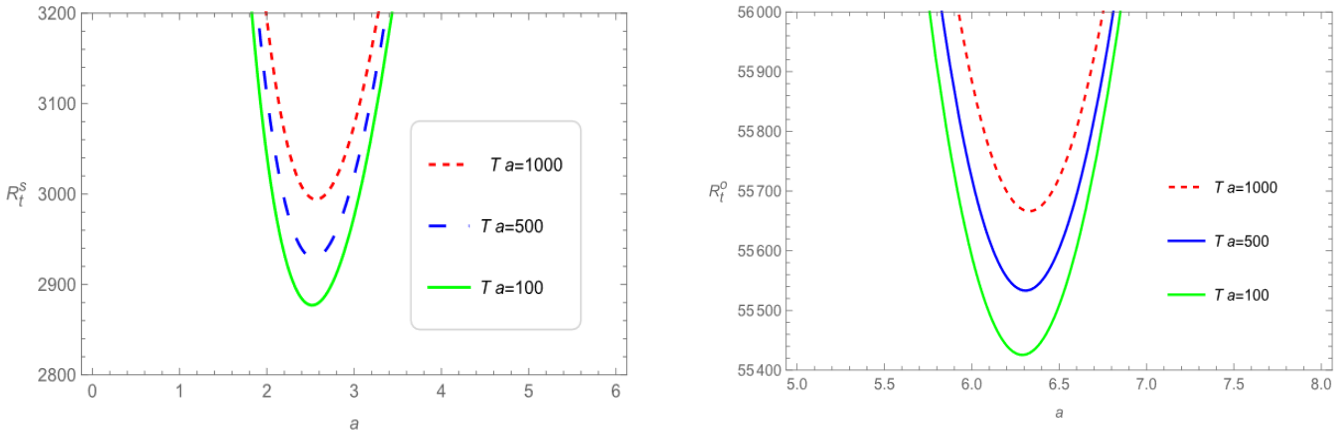
Fig. 3: (a) R_t^s vs a for various values of Λ with $R_i = 5$, $R_{ea} = 100$, $Da^{-1} = 100$ and $Ta = 10$ (for Stationary Convection); (b) R_t^o vs a for various values of Λ with $R_i = 5$, $R_{ea} = 100$, $Da^{-1} = 100$, $Pr = 5$, $\hat{\lambda} = 0.1$, $\Lambda = 1$, $M = 1$ and $Ta = 10$ (for oscillatory Convection).



(a) (b)

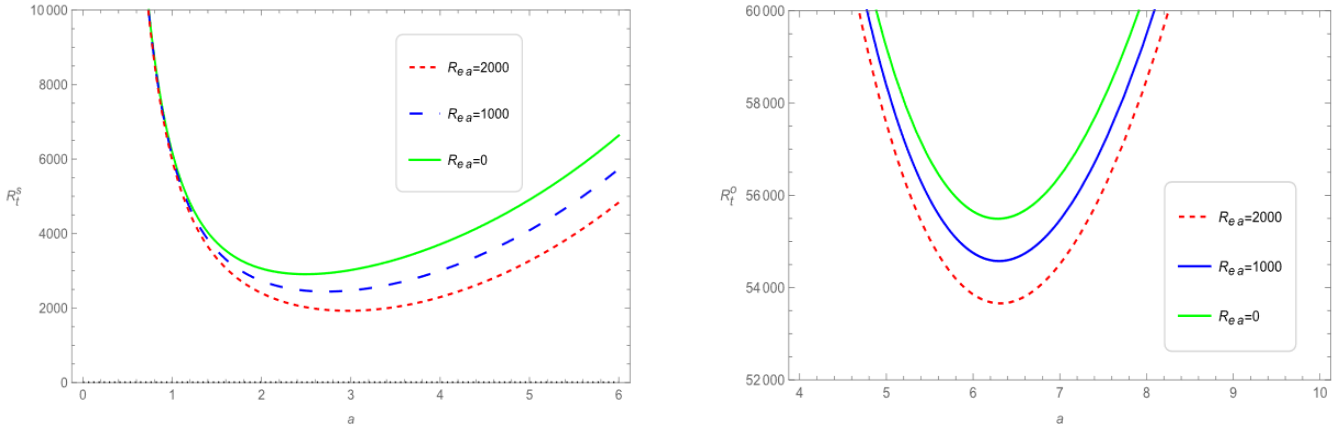
Fig. 4: (a) R_t^s vs a for various values of Da^{-1} with $R_i = 5$, $R_{ea} = 100$, $\Lambda = 1$ and $Ta = 10$ (for Stationary Convection); (b) R_t^o vs a for various values of Da^{-1} with $R_i = 5$, $R_{ea} = 100$, $Pr = 5$, $\hat{\lambda} = 0.1$, $\Lambda = 1$, $M = 1$ and $Ta = 10$ (for oscillatory Convection).

below) with $\Lambda = 1$, $R_i = 5$ and $Da^{-1} = 100$ for free boundaries. It is evident from the figure that for both cases, an increase in the value of Ta results into the increase in the value of a_c. Thus, the consequence is to contract the size of convective cells.



(a) (b)

Fig. 5: (a) R_t^s vs a for various values of Ta with $R_i = 5$, $R_{ea} = 100$, $\Lambda = 1$ and $Da^{-1} = 100$ (for Stationary Convection); (b) R_t^o vs a for various values of Ta with $R_i = 5$, $R_{ea} = 100$, $Pr = 5$, $\hat{\lambda} = 0.1$, $\Lambda = 1$, $M = 1$ and $Da^{-1} = 100$ (for oscillatory Convection).



(a) (b)

Fig. 6: (a) R_t^s vs a for various values of R_{ea} with $R_i = 5$, $\Lambda = 1$, $Da^{-1} = 100$ and $Ta = 10$ (for Stationary Convection); (b) R_t^o vs a for various values of R_{ea} with $R_i = 5$, $Da^{-1} = 100$, $Pr = 5$, $\hat{\lambda} = 0.1$, $\Lambda = 1$, $M = 1$ and $Ta = 10$ (for oscillatory Convection).

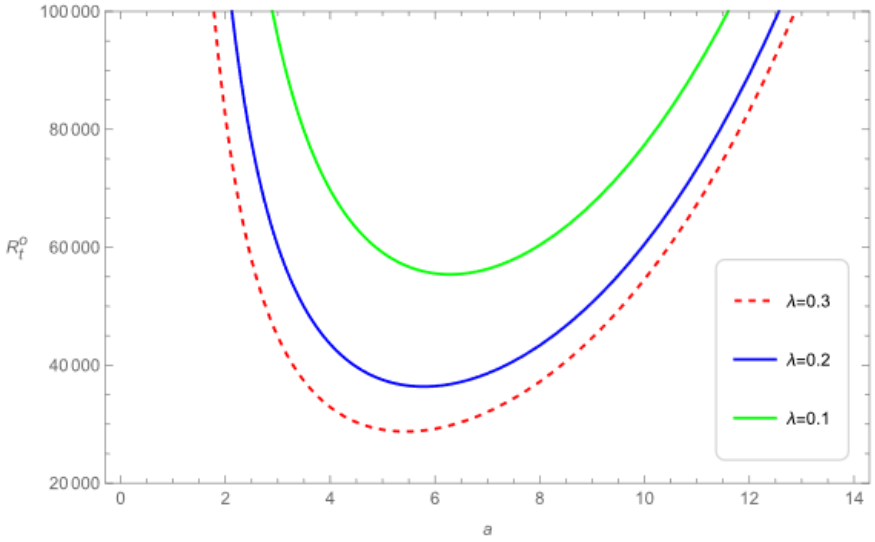


Fig. 7: R_t^o vs a for various values of $\hat{\lambda}$ with $R_i = 5$, $Da^{-1} = 100$, $Pr = 5$, $R_{ea} = 100$, $\Lambda = 1$, $M = 1$ and $Ta = 10$ (for oscillatory Convection).

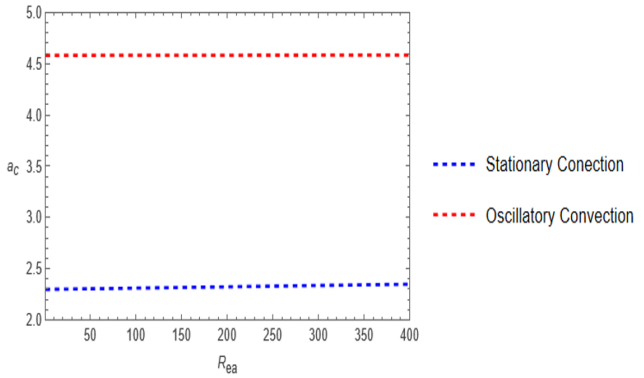


Fig. 8: The variation of a_c with R_{ea} for $\Lambda = 4$ with $R_i = 5$, $Da^{-1} = 100$, $Pr = 5$, $M = 1$ and $Ta = 10$.

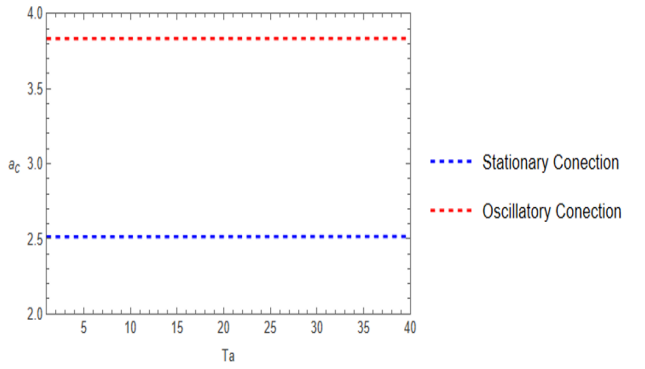
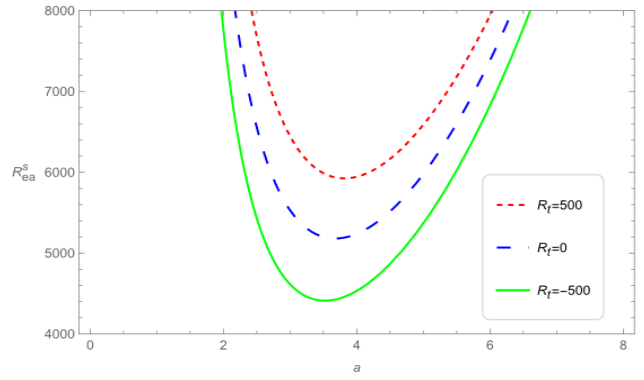
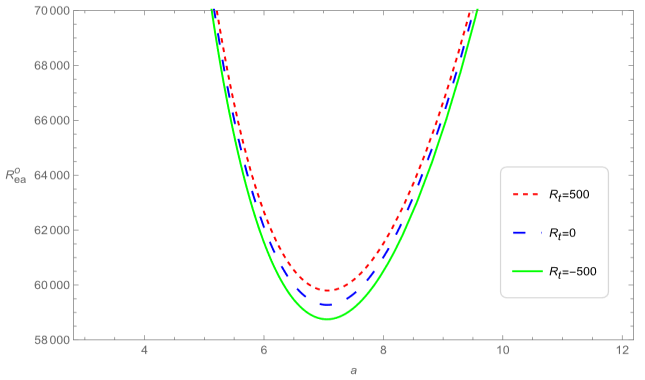


Fig. 9: The variation of a_c with Ta for $Da^{-1} = 100$ with $R_i = 5$, $Pr = 5$, $M = 1$, $\Lambda = 1$ and $R_{ea} = 100$.



(a)



(b)

Fig. 10: (a) R^s_{ea} vs a for various values of R_t with $R_i = 5$, $\Lambda = 1$, $Da^{-1} = 100$ and $Ta = 10$ (for Stationary Convection); (b) R^o_{ea} vs a for various values of R_t with $R_i = 5$, $Da^{-1} = 100$, $Pr = 5$, $\hat{\lambda} = 0.1$, $\Lambda = 1$, $M = 1$ and $Ta = 10$ (for oscillatory Convection).

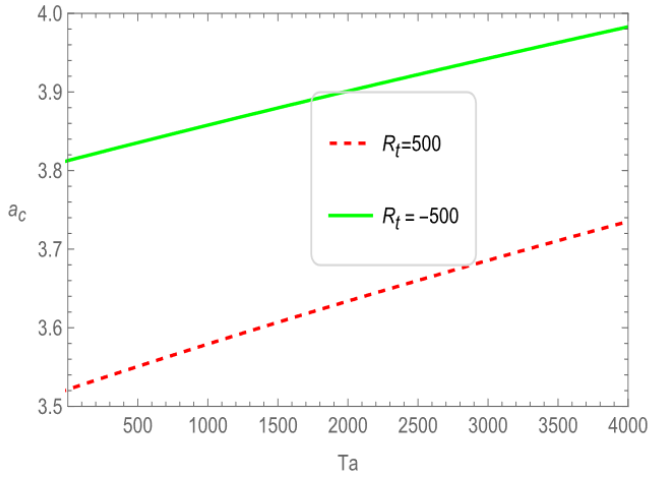


Fig. 11: The variation of a_c and Ta for various values of R_t with $R_i = 5$, $Da^{-1} = 100$, $\Lambda = 1$.

5 Conclusions

The simultaneous effect of vertical AC electric field, uniform rotation and internal heat source on the onset of Darcy-Brinkman convection in a rotating NSV viscoelastic dielectric fluid-saturated porous layer heated from below is investigated for free-free boundaries. The graph predicts that the criterion of onset of convection mainly depends upon the system's parameters. The following conclusions can also be drawn in the context of both stationary and oscillatory modes of convection:

- The inverse Darcy number Da^{-1}, the ratio of viscosities Λ and Taylor number Ta has a stabilizing effect on both stationary and oscillatory modes of convection.
- The electric Rayleigh number R_{ea} has a destabilizing effect on both stationary and oscillatory modes of convection.
- The Navier-Stokes-Voigt parameter $\hat{\lambda}$ has a destabilizing effect on the oscillatory mode of convection.

- The effect of the increase in electric Rayleigh number R_{ea}, inverse Darcy number Da^{-1} and Taylor number Ta is to contract the dimension of the convection cells, while increase in the ratio of viscosities Λ and internal Rayleigh number R_i to elongate the same.
- The size of convection cells is smaller when the system is heated from above compared to the system heated from below.
- Increasing inverse Darcy number Da^{-1} and the ratio of viscosities Λ has a destabilizing effect on the stationary convection depending on the strength of rotation.
- In contrast to heating from below, for both stationary as well as oscillatory modes of convection, when the system is heated from above, it shows a notable delay in the onset of instability. Hence, the above-mentioned facts predict an insight for the combined effect of AC-electric field and uniform vertical rotation on the stability of rotating NSV viscoelastic dielectric fluid saturated in a porous layer when heated from below or above subject to different boundary conditions.

Acknowledgment

Authors are indebted to the learned reviewer who carefully read the manuscript and gave very constructive comments which resulted to bring the manuscript in the present form.

References

A. I. Alsabery, R. Mohebbi, A. J. Chamkha, and I. Hashim. Effect of local thermal non-equilibrium model on natural convection in a nanofluid-filled wavy-walled porous cavity containing inner solid cylinder. *Chemical Engineering Science*, 201:247–263, 2019.

A. J. Badday and A. J. Harfash. Thermosolutal convection in a Brinkman–Darcy–Kelvin–Voigt fluid with a bidisperse porous medium. *Physics of Fluids*, 36:014119, 2024. doi: 10.1063/5.0186934.

B. S. Bhadauria and P. Kiran. Weakly nonlinear oscillatory convection in a viscoelastic fluid saturating porous medium under temperature modulation. *International Journal of Heat and Mass Transfer*, 77:843–851, 2014. doi: 10.1016/j.ijheatmasstransfer.2014.05.037.

A. J. Chamkha. Double-diffusive convection in a porous enclosure with cooperating temperature and concentration gradients and heat generation or absorption effects. *Numerical Heat Transfer, Part A: Applications*, 41(1):65–87, 2010.

A. J. Chamkha and C. Issa. Effects of heat generation/absorption and thermophoresis on hydromagnetic flow with heat and mass transfer over a flat surface. *International Journal of Numerical Methods for Heat & Fluid Flow*, 10(4):432–449, 2000. doi: 10.1108/09615530010327404.

S. Chandrasekhar. *Hydrodynamic and Hydromagnetic Stability*. Dover Publications, Inc., New York, 1981.

H. Demir. Rayleigh–Bénard convection of viscoelastic fluid. *Applied Mathematics and Computation*, 136(2-3):251–267, 2003. doi: 10.1016/S0096-3003(02)00036-X.

M. F. El-Sayed. Onset of electroconvective instability of Oldroydian viscoelastic liquid layer in Brinkman porous medium. *Archive of Applied Mechanics*, 78:211–224, 2008. doi: 10.1007/s00419-007-0153-x.

Y. Gaillard, P. S. B. Szabo, V. Travnikov, and C. Egbers. Thermo-electrohydrodynamic convection in a rotating shell with central force field. *International Journal of Heat and Mass Transfer*, 218, 2024.

R. S. R. Gorla, A. J. Chamkha, and A. M. Rashad. Mixed convective boundary layer flow over a vertical wedge embedded in a porous medium saturated with a nanofluid: Natural convection dominated regime. *Nanoscale Research Letters*, 6(207), 2011.

V. C. Ibezim, R. J. Poole, and D. J. Dennis. Viscoelastic fluid flow in microporous media. *Journal of Non-Newtonian Fluid Mechanics*, 296:104638, 2021. doi: 10.1016/j.jnnfm.2021.104638.

J. Kang, C. Fu, and W. Tan. Thermal convective instability of viscoelastic fluids in a rotating porous layer heated from below. *Journal of Non-Newtonian Fluid Mechanics*, 166(1-2):93–101, 2011. doi: 10.1016/j.jnnfm.2010.10.008.

J. Kumar, C. Kumari, A. Sharma, and J. Prakash. The onset of electrothermoconvection in a viscoelastic rotating dielectric fluid layer: Navier–Stokes–Voigt model. *Heat Transfer*, 2025. doi: 10.1002/htj.70131.

C. Kumari, J. Kumar, and J. Prakash. The onset of electrothermoconvection in a viscoelastic dielectric fluid layer with internal heat source: Navier–Stokes–Voigt model. *Technische Mechanik: European Journal of Engineering Mechanics*, 44(4), 2024. doi: 10.24352/UB.OVGU-2024-068.

T. Maekawa. Onset of natural convection under an electric field. *International Journal of Heat and Mass Transfer*, 35(3):613–621, 1992.

O. P. Matveeva. Model of thermoconvection of incompressible viscoelastic fluid of nonzero order. Computational experiment. *Bulletin of the South Ural State University. Series: Mathematical Modelling, Programming and Computer Software*, 6:134–138, 2013.

E. O. Odok, C. Israel-Cookey, and E. Amos. Onset of magnetoconvection in a rotating Darcy–Brinkman porous layer heated from below with temperature dependent heat source. *International Journal of Mathematics Trends and Technology*, 66, 2020. doi: 10.14445/22315373/IJMTT-V66I5P507.

A. P. Oskolkov. Initial-boundary value problems for equations of motion of Kelvin–Voigt fluids and Oldroyd fluids. *Proceedings of the Steklov Institute of Mathematics*, 179:159–180, 1987.

A. P. Oskolkov. Nonlocal problems for the equations of motion of Kelvin–Voight fluids. *Journal of Mathematical Sciences*, 75: 2058–2078, 1995. doi: 10.1007/BF02362946.

M. I. Othman. Electrohydrodynamic stability in a horizontal viscoelastic fluid layer in the presence of a vertical temperature gradient. *International Journal of Engineering Science*, 39(11):1217–1232, 2001. doi: 10.1016/S0020-7225(00)00092-6.

M. I. Othman and N. H. Sweilam. Electrohydrodynamic instability in a horizontal viscoelastic fluid layer in the presence of internal heat generation. *Canadian Journal of Physics*, 80(6):697–705, 2002. doi: 10.1139/p02-015.

M. I. Othman and S. A. Zaki. The effect of thermal relaxation time on a electrohydrodynamic viscoelastic fluid layer heated from below. *Canadian Journal of Physics*, 81(5):779–787, 2003. doi: 10.1139/p03-013.

A. Priyanshu and N. Deepika. Double diffusive convective instability in an anisotropic porous layer with Brinkman–Darcy–Kelvin–Voigt model: Vertical throughflow. *International Journal of Thermal Sciences*, 223, 2026.

K. R. Raghunatha and I. S. Shivakumara. Double-diffusive convection in a rotating viscoelastic fluid layer. *ZAMM – Journal of Applied Mathematics and Mechanics*, 101(4):e201900025, 2021. doi: 10.1002/zamm.201900025.

G. Rasool, A. J. Chamkha, T. Muhammad, A. Shafiq, and I. Khan. Darcy–Forchheimer relation in Casson type MHD nanofluid flow over non-linear stretching surface. *Propulsion and Power Research*, 9(2):159–168, 2020.

L. V. Reddy, R. Ragoju, S. Shekhar, and D. Yadav. Weakly nonlinear analyses on double-diffusive convection of Casson fluid in a porous medium with an internal heat and gravity modulation. *The European Physical Journal B*, 98(5):1–16, 2025. doi: 10.1140/epjb/s10051-025-00947-w.

P. H. Roberts. Electrohydrodynamic convection. *The Quarterly Journal of Mechanics and Applied Mathematics*, 22(2):211–220, 1969. doi: 10.1093/qjmam/22.2.211.

B. M. Shankar and I. S. Shivakumara. Stability of natural convection in a vertical layer of Navier–Stokes–Voigt fluid. *International Communications in Heat and Mass Transfer*, 144:106783, 2023. doi: 10.1016/j.icheatmasstransfer.2023.106783.

I. S. Shivakumara, M. S. Nagashree, and K. Hemalatha. Electrothermoconvective instability in a heat generating dielectric fluid layer. *International Communications in Heat and Mass Transfer*, 34(9-10):1041–1047, 2007. doi: 10.1016/j.icheatmasstransfer.2007.05.006.

I. S. Shivakumara, N. Rudraiah, and K. Hemalatha. Electrothermoconvection in a dielectric fluid layer in the presence of heat generation. *International Journal of Applied Mathematics*, 1(1):87–101, 2009.

I. S. Shivakumara, C. O. Ng, and M. S. Nagashree. The onset of electrothermoconvection in a rotating Brinkman porous layer. *International Journal of Engineering Science*, 49(7):646–663, 2011. doi: 10.1016/j.ijengsci.2011.02.010.

B. Shivaraj, P. G. Siddheshwar, and D. Uma. Effects of variable viscosity and internal heat generation on Rayleigh–Bénard convection in Newtonian dielectric liquid. *International Journal of Applied and Computational Mathematics*, 7(3):119, 2021. doi: 10.1007/s40819-021-01060-z.

H. Singh, C. Kumari, J. Kumar, and J. Prakash. The onset of electrothermoconvection in a dielectric viscoelastic Navier–Stokes–Voigt fluid in sparsely distributed porous medium. *Journal of Porous Media*, 2025. doi: 10.1615/JPorMedia.2025058170.

B. Straughan. Thermosolutal convection with a Navier–Stokes–Voigt fluid. *Applied Mathematics & Optimization*, 84(3): 2587–2599, 2021. doi: 10.1007/s00245-020-09719-7.

B. Straughan. Nonlinear stability for convection with temperature dependent viscosity in a Navier–Stokes–Voigt fluid. *The European Physical Journal Plus*, 138(5):438, 2023. doi: 10.1140/epjp/s13360-023-04055-5.

T. G. Sukacheva and O. P. Matveeva. On a homogenous thermoconvection model of the non-compressible viscoelastic Kelvin–Voight fluid of the non-zero order. *Journal of Samara State Technical University, Series Physical and Mathematical Sciences*, 21:33–41, 2010.

M. Takashima. The effect of rotation on electrohydrodynamic instability. *Canadian Journal of Physics*, 54(3):342–347, 1976. doi: 10.1139/p76-039.

P. Vadasz. Instability and convection in rotating porous media: A review. *Fluids*, 4(3):147, 2019. doi: 10.3390/fluids4030147.

D. Yadav, J. Wang, and J. Lee. Onset of Darcy–Brinkman convection in a rotating porous layer induced by purely internal heating. *Journal of Porous Media*, 20(8), 2017.